

Seasonal Distributions of Aeolian Iron Fluxes to the Global Ocean

Y. Gao,^{1,2} Y. J. Kaufman,³ D. Tanré,⁴ D. Kolber,¹ and P. G. Falkowski¹

Abstract. Among the factors affecting the photosynthetic rate of marine phytoplankton, aeolian iron (Fe) fluxes appear to be critical in several large regions of the global ocean. Here we present an analysis of *in situ* aerosol iron data obtained from a wide variety of marine locations to quantify the seasonal Fe inputs to the global ocean. When extrapolated to the global ocean, our results indicate strong seasonal variations in aeolian Fe fluxes in different oceanic basins. The predominant fraction of the Fe inputs enters the oceans in the Northern Hemisphere, with the summer flux rates ca. twice those of winter. The high Fe fluxes in the Northern Hemisphere are concentrated in low and mid-latitudes. With the promising new data from MODIS aboard the Terra satellite, the linkage between Fe fluxes and phytoplankton biomass and productivity may be soon further quantified.

1. Introduction

John Martin and colleagues (Martin and Gordon, 1988) hypothesized that in certain oceanic regions (high-nitrate, low chlorophyll - HNLC regions), the micronutrient, Fe, regulates phytoplankton growth. Fe fertilization experiments in the equatorial Pacific (Coale et al., 1996) and Southern Ocean (Boyd et al., 2000) provided unequivocal support of the Fe hypothesis. The results from these experiments also led to the suggestion that Fe fertilization could affect the cycles of other nutrients, especially nitrogen (Falkowski, 1997), which may further affect nitrogen fixing bacteria such as *Trichodesmium* (Capone et al., 1997) and the biomass specific rate of photosynthesis (Behrenfeld et al., 1996). Thus the delivery of iron to the ocean may cause changes in the global carbon cycles, in particular atmospheric CO₂. Indeed, the ~420 kyr ice core record from Vostok reveals a strong inverse relationship between dust loading (e. g., aeolian Fe) and atmospheric CO₂ (Petit et al., 1999). Fe-induced CO₂ uptake by oceanic biosphere may well interact with global climate on geological time scales (Broecker and Henderson, 1998).

The major source of Fe in the surface waters of the open ocean is aeolian dust delivered through long-range transport from arid continental regions (Duce et al., 1980). Model

results suggest that aeolian Fe is the major fraction of the total iron in the surface ocean (Fung et al., 2000). Duce and Tindale (1991) calculated the annual input of the total aeolian Fe to the global ocean to be $32 \times 10^{12} \text{ g yr}^{-1}$. Although these studies demonstrate the importance of Fe inputs, a detailed coupling of aeolian Fe fluxes and biological responses remains unclear. Since many biological processes are seasonally dependent, quantification of the total aeolian Fe deposition on a seasonal basis is needed to characterize the linkage.

As the first step to examining the seasonal linkage between aeolian Fe and phytoplankton productivity, we applied limited *in situ* aerosol data obtained in the marine boundary layer (MBL) to quantify seasonal Fe fluxes. Our goal was to establish the seasonal climatological distributions of Fe fluxes on a global scale. The preliminary results from this work will further support the exploration of the Fe input - oceanic biomass relationship and the development of oceanic biogeochemical models. Inevitably, however, this approach will always undersample the global ocean. To address this deficiency, we examined the potential application of remotely sensed dust detected by a Moderate Resolution Imaging Spectroradiometer (MODIS) onboard the Terra spacecraft (Kaufman et al., 1997; Tanré et al., 1997). Since dust absorption relates to its Fe content, the results can, in principle, be used to assist in real-time retrieval of dust properties from satellites to improve the Fe flux estimates.

2. Method

2.1. Iron Data Base

Seasonal Fe fluxes to the oceans were derived from a compilation of aerosol Fe or dust concentrations obtained from *in situ* measurements in the MBL at 73 sites representing a variety of marine locations. These include results from large-scale atmospheric networks, such as The Sea-Air Exchange Program in the Pacific (SEAREX, 1977-1986) and The Atmosphere-Ocean Chemistry Experiment in the Atlantic (AEROCE, 1988-1996). Among the oceanic sites are Barbados (13°N, 60°W), Bermuda (32°N, 65°W), Mace Head (53°N, 10°W), and Izana (28°N, 17°W) in the Atlantic, and Shemya (53°N, 174°E), Midway (28°N, 177°W), Oahu (21°N, 158°W), Eniwetok (11°N, 162°E), Fanning (4°N, 159°W), and Samoa (14°S, 171°W) in the Pacific. These sites provide long-term records of seasonal patterns of dust in vast areas of the world ocean. In addition, results from numerous individual investigations were also considered, covering other regions including the Western North Pacific (Gao et al., 1992), the Indian Ocean (Savoie et al., 1987), the Arabian Sea (Tindale and Pease, 1999), the Southern Ocean and the Mid-Atlantic Bight (Gao, unpublished). The Fe data used here were either from direct aerosol Fe measurements or estimated based on dust measurements, assuming that Fe accounts for 3.5% of the total dust mass (Taylor and McLennan, 1985).

P. G. Falkowski, Y. Gao, and D. Kolber, Institute of Marine and Coastal Sciences, Rutgers University, New Brunswick, NJ 08901. (email: falko@imcs.rutgers.edu, yuangao@splash.princeton.edu)

Y. J. Kaufman, NASA Goddard Space Flight Center, Greenbelt, MD 20771. (email: kaufman@climate.gsfc.nasa.gov)

D. Tanré, Laboratoire d'Optique Atmosphérique, Villeneuve d'Ascq, France. (email: Didier.Tanre@univ-lille1.fr)

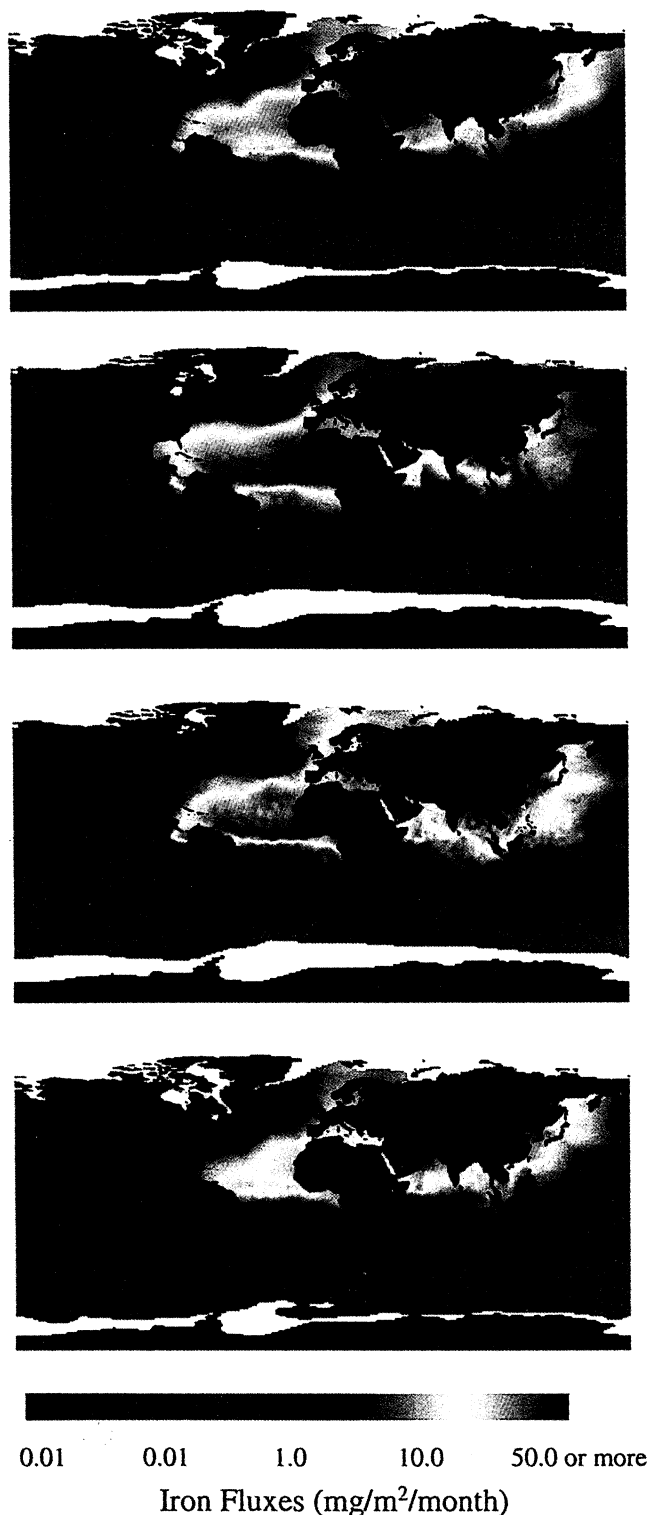


Figure 1. Seasonal distributions of atmospheric Fe fluxes to the global oceans.

Although chemical forms of Fe are important in oceanic biogeochemistry, we only considered total Fe in this work. Fe could be enriched in aerosols relative to its crustal abundance while the air mass advances over urban regions. Therefore, a small fraction of the total Fe may be of non-crustal origin. Moreover, we note that the *in situ* data obtained in the MBL with strong seasonal and spatial variations should be viewed

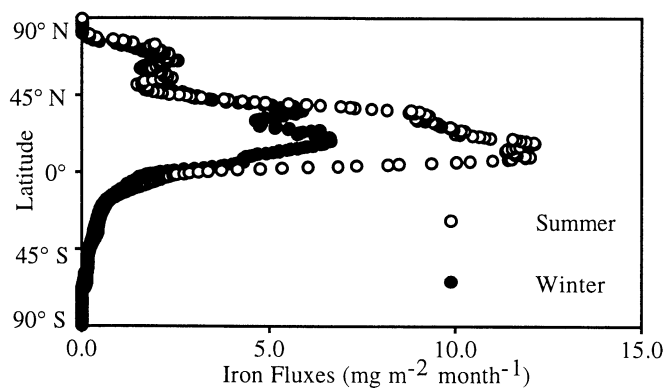


Figure 2. Summer-winter comparison of the atmospheric Fe fluxes between the Northern Hemisphere and the Southern Hemisphere.

as the end products of interactions of many processes including atmospheric transport and circulation.

2.2. Deposition Calculation

Using dry/wet deposition models which have been consistently used in the past (Duce and Tindale, 1991; Jickells and Spokes, 2000), we calculated Fe dry deposition through the use of a dry deposition velocity (V_d) and wet deposition with a scavenging ratio (S) that relates the Fe concentration in dust with that in precipitation. We used updated values for these exchange coefficients. For dry deposition, which is primarily a function of dust particle size, field measurements reveal that the mass median diameter (MMD) of dust tends to be relatively stable, ranging from one to several micrometers over the oceans (Prospero, 1995), with the V_d values ranging $0.4 - 2 \text{ cm s}^{-1}$. Comparison between dust deposition estimates



Figure 3. MODIS data for a dust episode off the Africa coast on 29 February, 2000. The left part of the image is a composite image of MODIS aerosol products. The right part is a simple true color image. Clouds are separated from non-cloudy regions and are represented with true color (gray). The aerosol product is represented with a blue color for an aerosol free atmosphere over the ocean. Dust replaces the blue with red and small particles with green. Yellow is a mixture of small particles (biomass burning or clay) and large dust particles.

Table 1. Seasonal and Annual Deposition of the Total Atmospheric Iron to the Major Ocean Basins.

Ocean Basin	Seasonal Fe Deposition (10^{12} g mon^{-1})				Annual Fe Deposition (10^{12} g yr^{-1})		
	Spring	Summer	Fall	Winter	This work (% of the total)	Duce and Tindale ^a	Jickells and Spokes ^b
North Pacific	0.28	0.17	0.34	0.20	3.0 (22%)	17	7.3
South Pacific	0.023	0.024	0.035	0.022	0.31 (2.3%)	1.4	0.67
North Atlantic	0.43	0.78	0.72	0.26	6.6 (48%)	7.7	6.0
South Atlantic	0.046	0.063	0.051	0.035	0.59 (4.3%)	0.84	0.46
Indian	0.21	0.15	0.26	0.18	2.4 (18%)	5.1	2.2
Antarctic	0.0062	0.0043	0.0078	0.0054	0.071 (0.52%)		
Arctic	0.0078	0.0099	0.018	0.0066	0.13 (0.93%)		
Mediterranean	0.068	0.043	0.048	0.022	0.54 (4.0%)		
Global Total					14	32	17

^a Estimates of Fe deposition of Duce and Tindale (1991), scavenging ratio = 200 for North Atlantic and 1000 for all others.

^b Based on dust estimates of Jickells and Spokes (2000), scavenging ratio = 200 for all ocean basins.

and sediment trap records in the Sargasso Sea suggests that a mean V_d value of 1.0 cm s^{-1} is more appropriate (Jickells and Spokes, 2000), and we chose 1.0 cm s^{-1} for V_d in our calculation. Based on the analysis of Jickells and Spokes (2000) considering results from a series of locations, we used 200 for the scavenging ratio. Precipitation fields were obtained from a global precipitation dataset of DASILVA SMD94 Climatology (01/1945–12/1993, $0.5^\circ \times 0.5^\circ$ spatial resolution) (da Silva et al., 1994). We recognize that there are large uncertainties in Fe flux estimates, mainly due to errors in exchange coefficients and global rainfall rates.

We calculated the total Fe fluxes and interpolated smoothly between discrete observations using natural-neighbor theory (Braun and Sambridge, 1995). We then ran four sets of calculations of the global Fe deposition for spring, summer, fall, and winter. The inter-hemispheric flux comparison between summer and winter was made based on these results.

3. Results and Discussions

3.1. Seasonal Patterns

The concentrations of aeolian Fe over the remote oceans are strongly affected by seasonal transport of dust from the deserts in the continents, which has direct impact on the seasonal and spatial distributions of iron fluxes to the oceans. Figure 1 indicates seasonal variations in Fe fluxes in different regions, ranging from <0.01 to $>80 \text{ mg m}^{-2} \text{ mon}^{-1}$. In the North Pacific, the highest Fe fluxes occur in the spring, due to the Asian dust transport by prevailing westerly winds. The largest fluxes are obtained in the spring over the Yellow Sea in the western North Pacific ($>50 \text{ mg m}^{-2} \text{ mon}^{-1}$), while the summer flux values are seen $<15 \text{ mg m}^{-2} \text{ mon}^{-1}$. This pattern is also reflected in the remote North Pacific. At Midway Island, the springtime Fe flux is $\sim 2.1 \text{ mg m}^{-2} \text{ mon}^{-1}$, four times the fluxes in the summer ($0.59 \text{ mg m}^{-2} \text{ mon}^{-1}$). These estimates agree reasonably well with directly measured dust fluxes at this location. Uematsu et al (1985) reported that the measured dust fluxes at Midway Island were $0.3 \mu\text{g cm}^{-2} \text{ d}^{-1}$ for the high dust season (Feb-Jun) and $0.08 \mu\text{g cm}^{-2} \text{ d}^{-1}$ during the clean season (July-Jan), which correspond to Fe fluxes of $2.8 \text{ mg m}^{-2} \text{ mon}^{-1}$ and $0.76 \text{ mg m}^{-2} \text{ mon}^{-1}$, respectively.

In the tropical and subtropical Atlantic, however, the highest Fe fluxes occur in the summer. Large quantities of Sahara dust are transported westward by trade winds during much of the year and this transport is enhanced during the summer (Prospero, 1995). At Barbados, the average Fe flux is

$\sim 45 \text{ mg m}^{-2} \text{ mon}^{-1}$ in the summer months, significantly higher than that in the winter ($\sim 20 \text{ mg m}^{-2} \text{ mon}^{-1}$). One feature in this region revealed by satellite images (Husar et al., 1997) is that the Saharan dust plume shows a seasonal latitudinal shift - $\sim 10^\circ$ - 15° farther north in the summer compared to the winter, driven by the migration of the inner-tropical convergence zone (ITCZ). However, this latitudinal shift does not appear in our Fe flux distributions. Since a satellite image reflects only the column integrated aerosol concentration, it may not be directly comparable to the Fe fluxes in the MBL, although the total Fe deposition is derived from the Fe concentration.

There is little seasonal variation in Fe fluxes in certain regions, such as the eastern South Pacific and the Southern Ocean where Fe fluxes are $<0.1 \text{ mg m}^{-2} \text{ mon}^{-1}$ throughout much of the year. This is due to the extremely low atmospheric concentrations of Fe over those regions, reflecting little influence by dust transport through the year.

3.2. Comparison of Seasonal Iron Fluxes between the Hemispheres

Figure 2 represents a comparison of the latitudinally averaged Fe fluxes (every 0.5° over the ocean) between summer and winter. We define the seasons based on the Northern Hemisphere. The averaged Fe fluxes in summer are higher than those in winter. The summer maximum of the Fe fluxes reaches $\sim 12 \text{ mg m}^{-2} \text{ mon}^{-1}$ between 5°N - 20°N , whereas the corresponding winter maximum is $\sim 7 \text{ mg m}^{-2} \text{ mon}^{-1}$. This highlights the seasonal differences in Fe inputs to the ocean on a global scale. Figure 2 also clearly indicates that the predominant fraction of the Fe fluxes enters the ocean in the Northern Hemisphere. From the equator to $\sim 50^\circ\text{N}$, the Fe fluxes range from $\sim 3 \text{ mg m}^{-2} \text{ mon}^{-1}$ to $\sim 12 \text{ mg m}^{-2} \text{ mon}^{-1}$. The high Fe fluxes concentrate on the low and mid-latitude regions, reflecting the influences of the major deserts located in those latitudinal bands, including arid and semiarid regions in Asia, North Africa, North America, India, and the Arabian peninsula. In the Southern Hemisphere, the Fe fluxes seldom reach $1 \text{ mg m}^{-2} \text{ mon}^{-1}$ in the areas south of the 15°S and remain $<0.1 \text{ mg m}^{-2} \text{ mon}^{-1}$ in the vast areas of the eastern South Pacific and the Southern Ocean.

An increase in the Fe fluxes occurs at high latitudes in the N. Hemisphere (60°N and above). High dust loading has been recorded in the Greenland ice core, linked with strengthened East Asian winter monsoon (Porter and An, 1995). Due to the lack of enough aerosol data in that region, the interpretation of the present-day Fe fluxes should be taken cautiously.

3.3. Total Iron Fluxes to the Global Ocean

In Table 1 we present a compilation of the total Fe deposition to the major ocean basins on seasonal and annual basis, including a comparison with other studies. In the North Atlantic, the highest Fe deposition occurs in summer ($0.78 \times 10^{12} \text{ g mon}^{-1}$) and the lowest in winter ($0.26 \times 10^{12} \text{ g mon}^{-1}$). A similar seasonal pattern also exists in the South Atlantic. Seasonal Fe deposition in the North Pacific reflects the high dust loading in the spring, with the total Fe deposition of $0.28 \times 10^{12} \text{ g mon}^{-1}$. Surprisingly total Fe deposition in the fall in the North Pacific also appears to be high, which could be due to both dust activities in East Asia and high wet deposition derived from high precipitation rates over the South China Sea. Thus large geographical variations of precipitation rates may significantly affect the total Fe deposition compared with the atmospheric concentration patterns. On a global basis, the North Pacific and the North Atlantic are the two oceanic basins where the atmospheric Fe deposition is high compared with the other basins, accounting for 22% and 48% of the total Fe deposition, respectively. Low Fe deposition is found in the South Pacific (2.3%) and polar regions, with 0.52% for the Antarctic and 0.93% for the Arctic.

3.4. Dust (or Fe) Identifications from Space: MODIS Results

Satellite remote sensing has proven to be a powerful tool in detecting the occurrence and distribution of aerosols on a global scale (Herman et al., 1997). However, it has been a challenge to identify the aerosol type and to estimate the dust contribution. Only recently have new algorithms been developed to distinguish between air masses with mainly dust and those with mainly pollution aerosols and to measure their separate column concentrations. Figure 3 shows a dust plume flowing over the west coast of Africa to the Atlantic obtained from MODIS on board NASA's Terra satellite launched in December 1999, which uses a multi-spectral approach to measure aerosol optical properties. Although it is not a final calibrated product, this is the first time that a satellite image could distinguish between dust (red in the image) and small aerosols (green in the image). This preliminary analysis demonstrates the potential of MODIS retrievals for dust that could be further used to infer the aeolian iron content.

Acknowledgments. We wish to thank R. A. Duce and M. Uematsu for the SEAREX data, R. Arimoto for the AEROCE data, and N. Kubilay for the Mediterranean data. We thank J. M. Prospero, N. Tindale, I. Tegen, and J. L. Sarmiento for comments. We thank Z. Kolber for assistance with the Fe flux maps. The manuscript was improved by constructive reviews from three anonymous reviewers. This work was supported by NASA EOS/IDS grant NAG 5-9340.

References

- Behrenfeld, M.J., A.J. Bale, Z.S. Kolber, J. Aiken, and P.G. Falkowski, Confirmation of iron limitation of phytoplankton photosynthesis in the equatorial Pacific Ocean, *Nature*, 383, 508-511, 1996.
- Boyd, P.W. et al., A mesoscale phytoplankton bloom in the polar Southern Ocean stimulated by iron fertilization, *Nature*, 407, 695-702, 2000.
- Braun, J., and M. Sambridge, A numerical method for solving partial differential equations on highly irregular evolving grids, *Nature*, 376, 655-660, 1995.
- Broecker, W.S., and G.M. Henderson, The sequence of events surrounding Termination II and their implications for the cause of glacial-interglacial CO_2 changes, *Paleoceanography*, 13, 352-364, 1998.
- Capone, D.G., J.P. Zehr, H.W. Paerl, B. Bergman, and E.J. Carpenter, Trichodesmium, a globally significant marine cyanobacterium, *Science*, 276, 1221-1229, 1997.
- Coale, K.H. et al., A massive phytoplankton bloom induced by an ecosystem-scale iron fertilization experiment in the equatorial Pacific Ocean, *Nature*, 383, 495-501, 1996.
- da Silva, A., A.C. Young, and S. Levitus, Atlas of Surface Marine Data 1994, NOAA Atlas NESDIS 6, US Department of Commerce, Washington, DC, 1994.
- Duce, R.A., and N.W. Tindale, Atmospheric transport of iron and its deposition in the ocean, *Limnol. Oceanogr.*, 36, 1715-1726, 1991.
- Duce, R.A., C.K. Unni, B.J. Bay, J.M. Prospero, and J.T. Merrill, Long-range atmospheric transport of soil dust from Asia to the tropical North Pacific: temporal variability, *Science*, 209, 1522-1524, 1980.
- Falkowski, P.G., Evolution of the nitrogen cycle and its influence on the biological sequestration of CO_2 in the ocean, *Nature*, 387, 272-275, 1997.
- Fung, I.Y., S.K. Meyn, I. Tegen, S.C. Doney, J.G. John, and J.K.B. Bishop, Iron supply and demand in the upper ocean, *Glob. Biogeochem. Cyc.*, 14, 281-295, 2000.
- Gao, Y., R. Arimoto, R.A. Duce, D.S. Lee, and M.Y. Zhou, Input of atmospheric trace elements and mineral matter to the Yellow Sea during the spring of a low-dust year, *J. Geophys. Res.*, 97, 3767-3777, 1992.
- Herman, J.R., P.K. Bhartia, O. Torres, C. Hsu, C. Seftor, and E. Celarier, Global distribution of UV-absorbing aerosols from Nimbus 7/TOMS, *J. Geophys. Res.*, 102, 16911-16922, 1997.
- Husar, R.B., J.M. Prospero, and L.L. Stowe, Characterization of tropospheric aerosols over the oceans with the NOAA advanced very high resolution radiometer optical thickness operational product, *J. Geophys. Res.*, 102, 16889-16909, 1997.
- Jickells, T.D., and L.J. Spokes, Atmospheric iron inputs to the ocean, in: *Biogeochemistry of Iron in Seawater* (Eds. D. Turner and K. A. Hunter), John Wiley & Sons, in press, 2000.
- Kaufman, Y.J., D. Tanre, H.R. Gordon, T. Nakajima, J. Lenoble, R. Frouin, H. Grassl, B.M. Herman, M. King, and P.M. Teillet, Passive remote sensing of tropospheric aerosol and atmospheric correction for the aerosol effect, *J. Geophys. Res.*, 102, 16815-16830, 1997.
- Martin, J.H., and R.M. Gordon, Northeast Pacific iron distributions in relation to phytoplankton productivity, *Deep-Sea Res.*, 35, 177-196, 1988.
- Petit, J.R., et al., Climate and atmospheric history of the past 420,000 years from the Vostok ice core, Antarctica, *Nature*, 399, 429-436, 1999.
- Porter, S.C., and Z. An, Correlation between climate events in the North Atlantic and China during the last glaciation, *Nature*, 375, 305-308, 1995.
- Prospero, J.M., The Atmospheric transport of particles to the ocean, in: *Particle Flux in the Ocean* (Eds. V. Ittekkot et al.), John Wiley & Sons, New York, 19-52, 1995.
- Savoie, D.L., J.M. Prospero, and R.T. Nees, Nitrate, non-sea-salt sulfate, and mineral aerosol over the northwestern Indian Ocean, *J. Geophys. Res.*, 92, 933-942, 1987.
- Tanré, D., Y.J. Kaufman, M. Herman and S. Mattoo, Remote sensing of aerosol over oceans from EOS-MODIS, *J. Geophys. Res.*, 102, 16971-16988, 1997.
- Taylor, S.R., and S.M. McLennan, *The Continental Crust: Its Composition and Evolution*, Blackwell Scientific, 312 pp, 1985.
- Tindale, N.W., and P.P. Pease, Aerosols over the Arabian Sea: Atmospheric transport pathways and concentrations of dust and sea salt, *Deep-Sea Res.*, 46, 1577-1595, 1999.
- Uematsu, M., R.A. Duce, and J.M. Prospero, Deposition of atmospheric mineral particles in the North Pacific Ocean, *J. Atmos. Chem.*, 3, 123-138, 1985.

¹ Institute of Marine and Coastal Sciences, Rutgers University, New Brunswick, NJ

² Also at Program in Atmospheric and Oceanic Sciences, Princeton University, Princeton, NJ

³ NASA Goddard Space Flight Center, Greenbelt, MD

⁴ Laboratoire d'Optique Atmosphérique, CNRS, Université de Sciences et Techniques de Lille, Villeneuve d'Ascq, France